International Journal of Disaster Risk Reduction 132 (2026) 105946

Contents lists available at ScienceDirect

International Journal of Disaster Risk Reduction

journal homepage: www.elsevier.com/locate/ijdrr

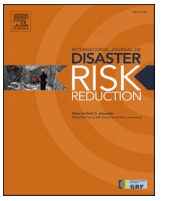

A nation-wide classification of the Italian Railway Network susceptibility to flood hazard

Gianluca Lelli [a,*], Serena Ceola [a], Alessio Domeneghetti [a], Adriana Galli [b], Edmondo Elisei [b], Alessandro Rinaldi [b], Armando Brath [a]

[a] Department of Civil, Chemical, Environmental, and Materials Engineering, Alma Mater Studiorum Università di Bologna, 40136, Bologna, Italy
[b] Technical Department, Rete Ferroviaria Italiana (RFI) S.p.a., Rome, Italy

ARTICLE INFO

Keywords:
Railways
Floods
Hazard
DEM
Time of concentration
Debris-flow

ABSTRACT

Floods pose significant threats to railway infrastructure, given their linear extension across diverse landscapes and frequent intersections with rivers. While European countries have developed Flood Risk Management Plans (FRMPs) following the EU Floods Directive, a comprehensive analysis of railway network flood susceptibility at national scale is still lacking for Italy. Here we develop a comprehensive flood hazard classification for the Italian Railway Network (IRN). Our methodology integrates flood hazard maps, railway infrastructure data, and digital elevation models to characterize flood hazard classes along flood-prone railway routes. The approach distinguishes between steep rapid, rapid and slow flood processes, based on topographical characteristics. Results demonstrate that, for the low probability flood hazard scenario (return period $\geq$500 years), 25.63 % of the IRN (4,523.4 km) exhibits flood susceptibility, with this proportion declining to 19.09 % and 9.77 % for medium and high flood hazard, respectively. By performing a regional analysis across seven hydrographic districts in Italy, a substantial spatial variability emerges, with the Po River district encompassing nearly half (47.5 %) of all flood-prone railway sections. Our analysis reveals also a marked predominance of rapid flood processes, characterized by values for the time of concentration $<$12 h. Our classification framework provides crucial insights for risk mitigation and resource allocation, relying exclusively on FRMPs and digital elevation models. The methodology presents a scalable approach applicable to other transportation networks and study areas, supporting infrastructure managers in developing targeted flood protection measures.

1. Introduction

Flooding represents one of the most devastating natural hazards worldwide, causing extensive damage to critical infrastructure systems. Approximately 27 % of all road and railway assets are exposed to at least one natural hazard, with flooding accounting for 73 % of expected annual damages to transport infrastructure, estimated at 3.1 to 22 billion US dollars globally [1]. Railways are particularly vulnerable to flooding due to their unique characteristics and operational requirements [2]. Railway networks are extensive linear infrastructures that intersect with numerous river courses, floodplains, and areas prone to surface water accumulation, making them susceptible to various flood scenarios. The 2013 floods in Central Europe, for example, caused over 84 million US dollar

* Corresponding author.
E-mail address: gianluca.lelli2@unibo.it (G. Lelli).

https://doi.org/10.1016/j.ijdrr.2025.105946
Received 12 September 2025; Received in revised form 19 November 2025; Accepted 1 December 2025
Available online 2 December 2025

damages to Austria's Federal Railways [3]. In China, railway operations are disrupted by flooding for an average of 1,125 h per year [4]. These events lead to substantial repair costs and other losses, such as service interruptions, passenger delays, and additional logistics efforts. Indirect damages may surpass direct ones, as demonstrated by the 2007 UK floods where indirect economic losses (1.5 billion UK pounds) exceeded direct damages (1.2 billion UK pounds) in the affected regions [5]. Railway infrastructure faces multiple damage mechanisms during floods. The most common scenario involves embankment overtopping, where flood waters exceed railway embankments and cause section washout. More severe scenarios include embankment instability from water infiltration, foundation scour that compromises structural integrity, and trains colliding with debris-flows. These disruptions spread through interconnected systems, affecting energy distribution, healthcare services, and broader transport networks [6]. Climate change is likely to intensify these risks globally [7], with Italy expected to face approximately 8.9 billion euro annually by the 2080s, i.e., among the highest projected climate damages in Europe [8]. For these reasons, flood hazard classification becomes crucial for effective railway management.

Different flood characteristics require distinct protection strategies, with two factors proving particularly critical: flood wave velocity, which impacts on the available warning time and emergency response time, and debris-flow potential, which affects impact severity and recovery duration. Fast-moving flash floods, typical of mountainous areas, allow little early warning compared to slower inundations in floodplains. Railway operators must therefore adopt regional approaches, ranging from speed restrictions to preventive closures. In Italy, this complexity is evident across railway networks spanning from the Alpine arc to the Po River basin [9,10]. Furthermore, debris-flows represent an additional hazard, especially at river crossings and in steep terrains. These events can obstruct railway lines, damage infrastructure through impact forces, and cause long-lasting service disruptions. Understanding where debris mobilization is likely to occur enables operators to apply specific protective measures and design early warning systems. Recently, Marchesini et al. (2024) [11] assessed railway exposure to rapid flow-like landslides (debris-flows, mudflows) at the Italian scale using detailed susceptibility mapping and runout modeling. Additional examples of such systems in Alpine regions are discussed by Nester et al. [12], while broader frameworks for vulnerability assessment are proposed by Hong et al. [13].

The European Union's Floods Directive (2007/60/EC) requires European countries to map flood-prone areas and develop comprehensive management plans, which are updated every six years. This Directive has become increasingly urgent as extreme weather events intensify across Europe [14], placing greater stress on railway infrastructure [7,8]. Italy has developed Flood Risk Management Plans (FRMPs) as required, providing flood hazard mapping for major river systems [15]. However, while certain countries have developed comprehensive railway flood assessments, see e.g., China's national network analysis [4], Italy lacks a comparable systematic evaluation at the national scale, since railway flood susceptibility was assessed only across specific Italian regions [16,17]. However, despite these advances, there is no nation-wide study that estimates and classifies the percentage of the Italian Railway Network (IRN) at risk of flood, by considering different flood hazard scenarios and providing a detailed hydrological characterization. Without this knowledge, infrastructure managers cannot prioritize which railway sections need urgent protection neither develop targeted monitoring strategies.

Different approaches exist for assessing flood risks across entire railway networks, from detailed hydrodynamic modeling to simplified geomorphological methods based on Digital Elevation Models (DEM). Detailed hydrodynamic models offer high accuracy for flood depths, velocities, and inundation extents. For instance, Zakaria et al. [18] combined traditional HEC-RAS modeling with remotely sensed data and machine learning to develop automated daily flood prediction for railway corridors, addressing operational needs beyond the design flood events typically generated by hydraulic models. However, implementing these models requires considerable computational resources, extensive high-resolution data (1-m DEMs, detailed bathymetry, calibration datasets), and significant time investments. While these approaches are highly accurate for specific locations, they are not applicable to national-scale railway networks. DEM-based approaches offer instead a practical alternative for large-scale flood hazard assessment. They are more adaptable and faster while still providing valuable insights for infrastructure planning, depending on the type and resolution of the employed DEM. For instance, Varra et al. [16] integrated multiple DEM-derived topographic and hydrological factors through GIS-based multi-criteria analysis to map flood susceptibility for railway infrastructure in Southern Italy, demonstrating the applicability of simplified DEM-based methods for railway-specific assessments in data-scarce environments. While general methods exist for evaluating flood impacts on transport networks [19], railways need specialized approaches because of their unique construction characteristics and operational requirements [7]. This study adopts a DEM-based procedure for flood hazard classification of railway infrastructure across Italy. We develop and analyze an integrated dataset combining updated nationwide flood hazard maps from flood risk management plans, railway infrastructure data, and high resolution (25 m) EU-DEM, building upon the established classification framework by Samela et al. [17]. While this framework was validated on regional scales (~200–250 km) [17], our study represents the first nation-wide application to the entire Italian Railway Network (~17,650 km). The methodology incorporates critical morphological and hydrological factors including river slope, time of concentration, and debris-flow potential [20,21] through Flood Hazard Classes (FHCs). National-scale mapping through a consistent and uniform approach is essential for providing railway operators with the key elements needed to evaluate critical sections, establish intervention priorities, and implement real-time event management measures. This is particularly important given that flood processes are characterized by different velocities and response times that directly influence operational safety and system management strategies.

2. Data and methods

We adopt the methodology developed by Samela et al. [17] in order to characterize flood hazard classes associated with flood-prone sections of the Italian Railway Network (IRN). This procedure involves identifying flood-prone railway network sections, the corresponding river network, contributing area, river slope, time of concentration, and debris-flow proneness, as detailed below.

The input data for this analysis consist of three elements: (i) Flood Risk Management Plans (FRMPs), delineated by seven hydrographic districts across Italy, (ii) the Italian Railway Network (IRN), and (iii) a Digital Elevation Model (DEM).

The European Floods Directive 2007/60/EC requires river basin authorities across Europe to delineate FRMPs, which identify areas impacted by flood events for three hazard scenarios, namely H1, H2 and H3, associated with different frequencies. H1 represents low probability events with a return period (T) up to 500 years, H2 describes events with a medium probability (T = 100–200 years), and H3 refers to events with a high probability (T = 20–50 years). According to the EU Floods Directive, FRMPs across Italy are delineated by seven hydrographic districts (Table 1) [15]. Even though minor streams are typically overlooked, the most recent FRMPs dating back to 2020 provide the official flood hazard information across Italy (Fig. 1). However, it should be acknowledged that FRMP data exhibit substantial heterogeneity in terms of quality, density, and mapping methodology across the seven hydrographic districts. Different River Basin Authorities adopted different approaches, ranging from 1D and 2D hydraulic models to geomorphological and historical approaches [22]. This cartographic heterogeneity may introduce uncertainty in our classification framework, which we address by integrating FRMP data with complementary DEM-based geomorphic analyses.

As previously mentioned, flood-prone areas identified through FRMPs need to be intersected with the geographical location of the railway network. The Italian Railway Network (IRN), as characterized by Rete Ferroviaria Italiana (RFI), comprises 3,429 sections totaling approximately 17,650 km (mean length 5.17 km, median 4.40 km), with 91.51 % of sections shorter than 10 km and 57.95 % under 5 km. The dataset employed consists of a linear shapefile representing railway lines, where each section has a unique identifier. This identifier is used as the basis for section management and for automating the methodology.

In order to derive key hydrologic and geomorphic characteristics associated to flood-prone IRN sections, the EU-DEM digital elevation model with 25 m resolution [23,24] is employed. To identify flood-prone railway sections, the IRN is overlapped with flood hazard scenarios as defined in the FRMPs. Since flood hazard maps associated with different frequencies may overlap, a single railway section may be exposed to multiple flood hazard scenarios (see Fig. 1 as an example). Next, for each flood-prone railway section, Representative Points (RPs) are determined from the intersection between the river network and the flood-prone railway section.

We derive the river network from the EU-DEM, which is first hydrologically conditioned by removing sinks and depressions. Then flow directions are calculated using the D8 flow routing algorithm [25]. Channel initiation is identified using a combined drainage area and slope criterion following the general framework of Montgomery and Foufoula-Georgiou (1993) [26]: $A \times S^{\theta} > K$ where A is the contributing drainage area [m^2], S is the local slope [−], θ is an empirically calibrated exponent, and K is the threshold constant [m^2]. We adopt $\theta = 1.7$ and $K = 10^5$ m^2 from Giannoni et al. (2005) [27], who developed an objective procedure for defining area-slope threshold values through geomorphological analysis of drainage networks. These parameter values were validated against six representative railway catchments and the EU-Hydro hydrographic network [24] before the nation-wide application. From this hydrological characterization, we delineate upstream basins and calculate important terrain parameters such as river slopes and contributing areas.

RPs are assigned at river-railway intersections, while for railway sections in flood-prone areas without direct river crossings, RPs are determined from the identification of the closest river point along the steepest descent path. For railway sections with multiple river intersections, only the most downstream intersection is considered, which represents the point with the largest flow accumulation area. The upstream river basin is then delineated for each RP using EU-DEM data, representing the contributing area for each flood-prone railway section. Each RP is then associated to a river slope, computed using an eight-direction gradient method, which considers the elevation difference and the distance between the RP cell with respect to its eight neighbors. The steepest downward gradient is selected as the final slope value. For each RP, we compute the time of concentration T_c [hour], defined as the period of time required for storm runoff to flow from the most remote part of a river basin to the outlet [28]. Several empirical formulas, with varying degrees of complexity and applicability, allow for the estimation of T_c. In this study, we employ Giandotti formula [29], which incorporates relevant river basin characteristics and is expressed as follows:

$$T_c = \frac{4\sqrt{A} + 1.5L}{0.8\sqrt{H_{mean} - H_{min}}} \quad (1)$$

where A is the contributing or basin area [km^2], L is the length of the main flow path [km], and H_{mean} and H_{min} are the average and minimum elevations of the basin [m a.s.l.], respectively. L is calculated as the cumulative distance along the flow path (D8) from the RP to the most upper point of the identified hydrographic network. H_{mean} is derived by calculating the arithmetic mean of the DEM values

Table 1
Flood-prone areas [km^2] and flood-prone railway network [km] according to the FRMP scenarios for each hydrographic district across Italy.

Hydrographic District	H1 [km^2]	H2 [km^2]	H3 [km^2]	H1 Flood-prone IRN [km]	H2 Flood-prone IRN [km]	H3 Flood-prone IRN [km]
Po River	21,419.2	15,584.2	6,338.3	2,148.6	1,523.3	602.6
Eastern Alps	5,637.3	3,405.9	2,225.5	435.4	341.9	165.0
Northern Apennines	4,959.1	2,848.1	1,464.5	658.6	433.5	260.8
Central Apennines	2,132.9	1,334.8	776.9	414.6	340.5	227.6
Southern Apennines	5,995.3	5,565.2	4,219.8	696.5	605.9	365.8
Sicily	584.1	507.6	407.2	73.9	56.1	49.9
Sardinia	1,674.9	973.2	825.9	95.7	67.2	53.0
Italy	**42,402.8**	**30,219**	**16,258.1**	**4,523.4**	**3,368.5**	**1,724.7**

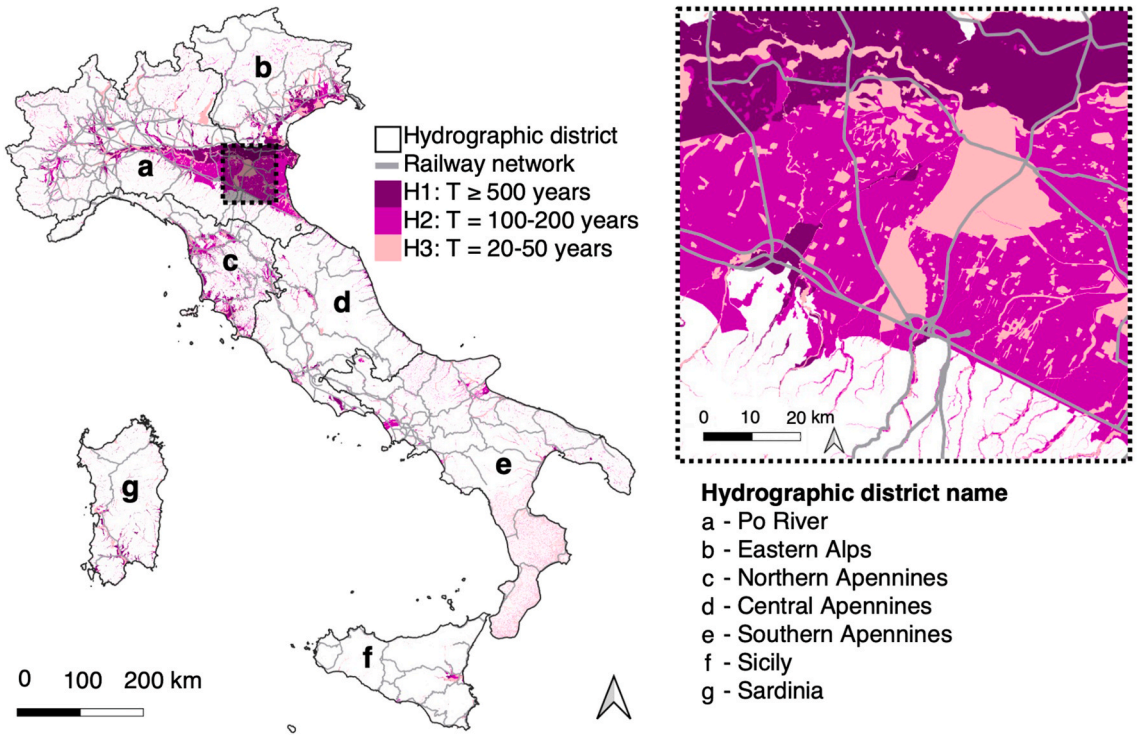

Fig. 1. Spatial representation of flood hazard scenarios and railway network across seven hydrographic districts in Italy. The cumulative flood hazard scenarios are shown in 3 shades of purple, where flood-prone areas according to H1 should embed also H2 and H3 flood-prone areas. The railway network is shown as a bold grey line. The boundaries of the seven hydrographic districts are labeled with letters and highlighted with a bold black line. The black dashed box represents a zoom-in of the area around the city of Bologna in the Po River hydrographic district.

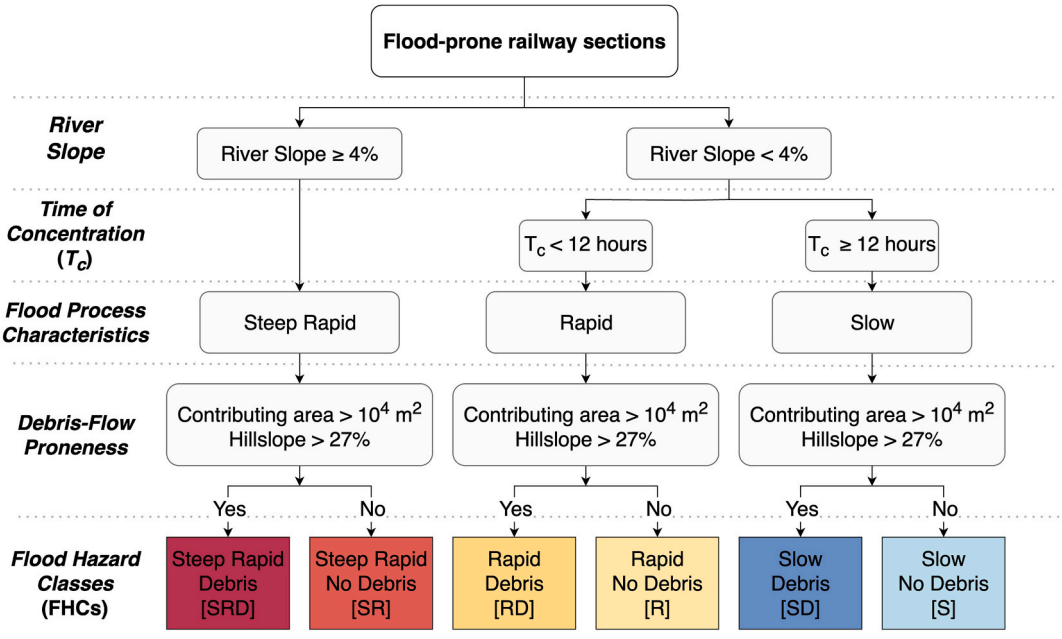

Fig. 2. Tree diagram illustrating the methodology towards the classification of flood-prone railway network sections and the corresponding Flood Hazard Classes (FHCs) derived from river slope, time of concentration, and debris-flow proneness (diagram re-elaborated from Samela et al. [17]).

across all pixels within the basin. The H_{min} is defined as the raw value of the DEM in the RP pixel. Developed in 1934, Giandotti formula (1) was initially calibrated for river basin areas ranging from 170 to 70,000 km^2. Recent studies have confirmed the applicability of the formula also in river basins exceeding the calibration threshold [30–32]. For the identified flood-prone sections, we also consider debris-flow proneness, being a significant hazard to railway infrastructure, particularly in areas characterized by critical slope gradients and loose sediment. These rapid mass movements are typically triggered by intense rainfall events, even those of short duration, and are known for their sudden onset. In identifying potential debris-flow source areas, topographical parameters derived primarily from DEM play a crucial role [20,33]. The hillslope gradient is computed for the entire basin area using the D8 method, previously introduced. Debris-flow-prone areas are identified when they simultaneously meet these criteria: (i) the contributing area exceeds 10^4 m^2, representing a threshold size for debris-flow initiation [26,34,35]; (ii) the hillslope gradient is between 27 % and 143 % (equivalent to 15°–55°) [36,37], representing the range where debris-flows typically develop; (iii) the location lies within a 1-km buffer from the railway line [38], establishing a practical limit for potential impact assessment. According to Samela et al. (2023) [17], river slope, time of concentration, and debris-flow proneness are combined to define six Flood Hazard Classes (FHCs) for the flood-prone railway sections. The first distinction in the flood hazard classification is river slope, with a threshold of 4 % (Fig. 2). This threshold, derived from empirical evidence and internal analyses of the Italian Railway Network characteristics, distinguishes between steeper (≥4 %) and less steep slope processes (<4 %), as it effectively discriminates between different hydrological response types. For rivers with a slope <4 %, a second classification is based on the time of concentration (T_c): rivers with $T_c < 12$ h are classified as rapid rivers, while rivers with $T_c \geq 12$ h are labeled as slow rivers. This 12-h threshold is defined in collaboration with RFI considering operational requirements for emergency response and flood mitigation actions. The debris-flow proneness parameter further subdivides each flood process category. Since potential debris-flow sources within flood-prone areas may compound the inundation hazard, we include the previously defined debris-flow proneness criteria following Samela et al. (2023) [17]. This rapid screening uses simplified topographic criteria, rather than the detailed debris-flow modeling employed by dedicated landslide studies [11].The study considers the following classification: rivers with slope ≥4 % are classified as Steep Rapid with Debris (SRD) when debris-flow prone conditions are met, and as Steep Rapid No Debris (SR) otherwise. For rivers with slope <4 % and $T_c < 12$ h, the classification yields Rapid with Debris (RD) in presence of debris-flow prone conditions, and Rapid No Debris (R) in the case of their absence. Finally, rivers with slope <4 % and $T_c \geq 12$ h are categorized as Slow with Debris (SD) when debris-flow prone conditions exist, and as Slow No Debris (S) otherwise.

3. Results: Flood hazard classification of the Italian Railway Network

To identify flood-prone railway sections, we intersect the Italian Railway Network (IRN) with flood hazard scenarios as defined in the FRMPs. The analysis reveals significant sections exposed to flood hazard across different scenarios. In the low probability scenario (H1, return period T ≥ 500 years), 25.63 % of IRN (4,523.4 km) is potentially affected by flooding (Table 2). Since flood hazard scenarios are cumulative, this value decreases to 19.09 % (3,368.5 km) in the medium probability scenario (H2, T equal to 100–200 years, see Table 1 and Table S1 in the Supplementary Tables) and further reduces to 9.77 % (1,724.7 km) in the high probability scenario (H3, T equal to 20–50 years, Table 1 and Table S2 in the Supplementary Tables).

Next, by overlapping the DEM-derived river network and the flood-prone railway sections, we identify Representative Points (RPs), which represent the outlet of river basins potentially affecting railway sections. Results show that the number of RPs decreases across scenarios, with 1,756, 1,605, and 1,251 RPs identified for scenarios H1, H2, and H3, respectively. In what follows, we provide a detailed description according to the worst-case scenario, i.e., H1 (Fig. 3). Relevant comments for H2 and H3 scenarios are available in the Supplementary Material. The analysis highlights substantial regional differences in the occurrence of RPs across the seven hydrographic districts (Fig. 3). The Po River district emerges as the most affected area, containing nearly half (45.16 %) of all RPs. Notable impacts also appear in the Southern and Northern Apennines, accounting for 17.31 % and 12.3 % of RPs, respectively. The Eastern Alps and Central Apennines show a lower occurrence, each representing about 9–10 % of RPs, while Sardinia and Sicily are the least affected, with 2.9 % and 1.99 %, respectively.

From the identification of RPs, we estimate relevant hydrologic and geomorphic characteristics (i.e., contributing area and time of concentration). The contributing area of rivers that intersect flood-prone IRN sections presents a sizeable variability across Italy (Fig. 4a), with larger contributing areas concentrated in the Po River hydrographic district and smaller ones typical of central and

Table 2
Flood-prone sections of the Italian Railway Network for each hydrographic district across Italy (in km and % of the network within the districts) and associated Flood Hazard Classes according to the low probability flood hazard scenario (H1).

Hydrographic District	Flood-prone IRN [km]	Flood-prone IRN [%]	Flood Hazard Classes (FHCs) [%]					
			SRD	SR	RD	R	SD	S
Po River	2,148.6	38	3.7	5.7	22.4	40.8	7.3	20.1
Eastern Alps	435.4	23	14.5	5.2	33.8	17.4	15.3	13.9
Northern Apennines	658.6	33	1.4	2.3	33.4	48.0	6.2	8.7
Central Apennines	414.6	18	5.7	2.9	30.3	43.0	8.1	10.0
Southern Apennines	696.5	18	4.1	3.5	31.2	30.8	20.6	9.8
Sicily	73.9	5	1.3	1.0	31.1	26.4	30.6	9.7
Sardinia	95.7	22	0.0	3.3	19.4	62.3	7.4	7.7
Italy	**4,523.4**	**26**	**4.5**	**4.4**	**27.3**	**38.5**	**10.4**	**14.9**

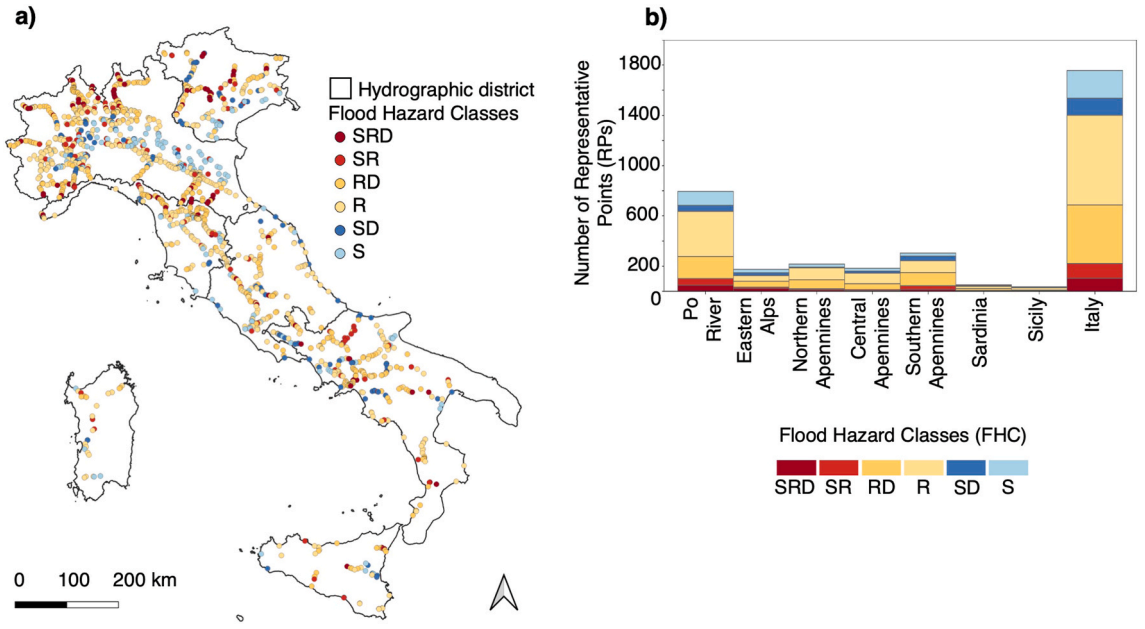

Fig. 3. Spatial and frequency distribution of Flood Hazard Classes (FHCs) attributed to Representative Points (RPs) according to the low probability flood hazard scenario (H1). (a) Geographical classification. (b) Frequency distribution across hydrographic districts.

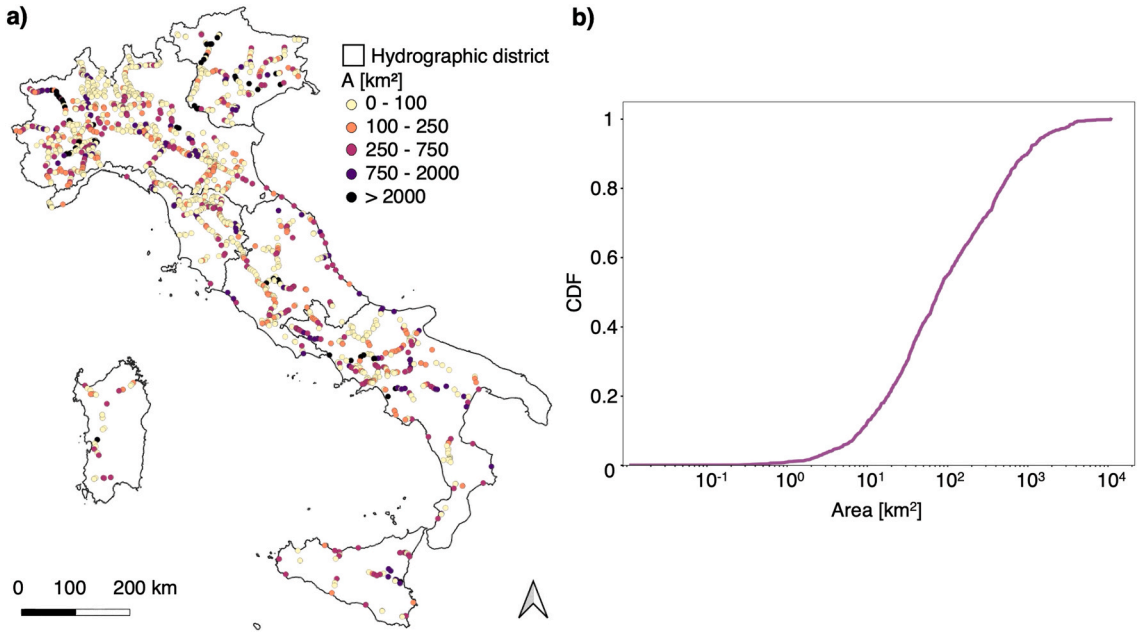

Fig. 4. Spatial and statistical distribution of the contributing area of river basins identified from the river-railway intersection according to the low probability flood hazard scenario (H1). (a) Representative Points (RPs i.e., the river basin outlet) classified by the contributing area. (b) Cumulative distribution function of contributing areas to RPs.

southern Italy. In scenario H1, contributing areas range from 0.01 km^2 to 10,842.58 km^2. From the cumulative distribution function (Fig. 4b), approximately 75 % of the basins have contributing areas smaller than 200 km^2 (median and mean values equal to 76.18 km^2 and 369.80 km^2, respectively). Similar statistical patterns are observed in scenarios H2 and H3, despite the reduction in the number of RPs (Supplementary Figures S3 and Figure S4). Contributing areas tend to increase from Steep Rapid classes (SRD, SR) to Slow classes (SD, S), as shown in Fig. 5a. Debris-flow prone basins (SRD, RD, SD) show larger contributing areas than non-debris-flow basins (SR, R, S), likely because larger basins have higher probability of containing hillslope portions meeting the debris-flow initiation criteria.

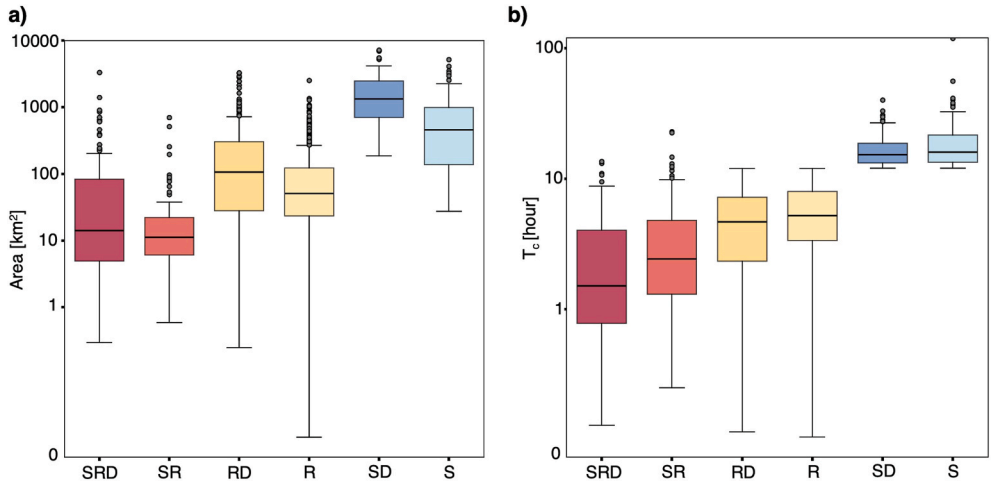

Fig. 5. Boxplot analysis of relevant hydrologic and geomorphic characteristics across different Flood Hazard Classes (FHCs) according to the low probability flood hazard scenario (H1). (a) Contributing areas associated to Representative points RPs (km^2). (b) Time of concentration (T_c) associated to RPs (hour).

A sizeable spatial variability of the time of concentration (T_c) associated with RP is found (Fig. 6a). For H1 scenario, values range from 0.1 to 119 h, with short (0–4 h) and moderate (4–12 h) T_c values widely distributed. Approximately 80 % of RPs have T_c values shorter than 20 h, with median and mean value equal to 5.99 and 7.72 h, respectively (Fig. 6b). Short T_c values are predominantly distributed across the Alps and the Apennines, reflecting a steeper topography and smaller contributing areas characteristic of these regions. In contrast, longer T_c values are mainly concentrated across the Po River hydrographic district, consistent with larger and less steep contributing areas. As expected, T_c values systematically increase from Steep Rapid classes (SRD, SR) to slow classes (SD, S), as shown in Fig. 5b.

We further distinguish flood processes between rapid (including both Steep Rapid and Rapid) and slow flood processes (see Fig. 2) and find that the Italian territory presents a clear predominance of rapid flood processes. Similar statistical patterns are observed in scenarios H2 and H3, despite the reduction in the number of RPs (Supplementary Fig. S5 and S6). Furthermore, RPs associated with shorter T_c values display greater variability in terms of FHCs, while RPs with longer T_c show more uniform distributions. Debris-flow prone river basins (SRD, RD, SD) are characterized by smaller T_c values compared to those without debris-flow proneness (SR, R, S).

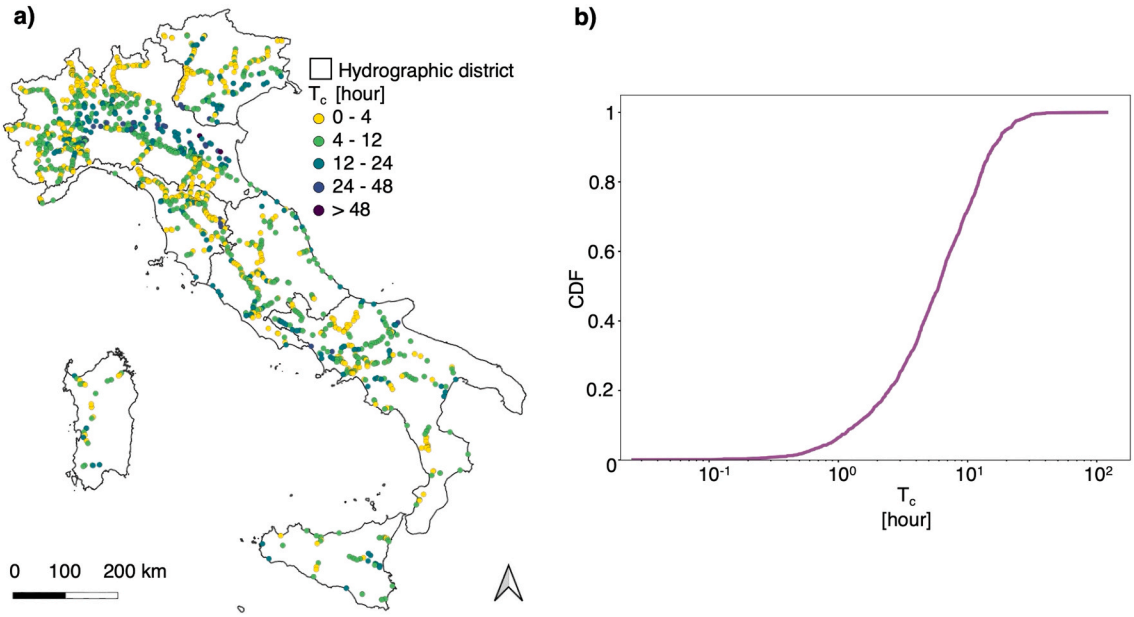

Fig. 6. Spatial and statistical distribution of the time of concentration of representative points (RPs) identified from the river-railway intersection according to the low probability flood hazard scenario (H1). (a) RPs classified by the time of concentration. (b) Cumulative distribution function of time of concentration values.

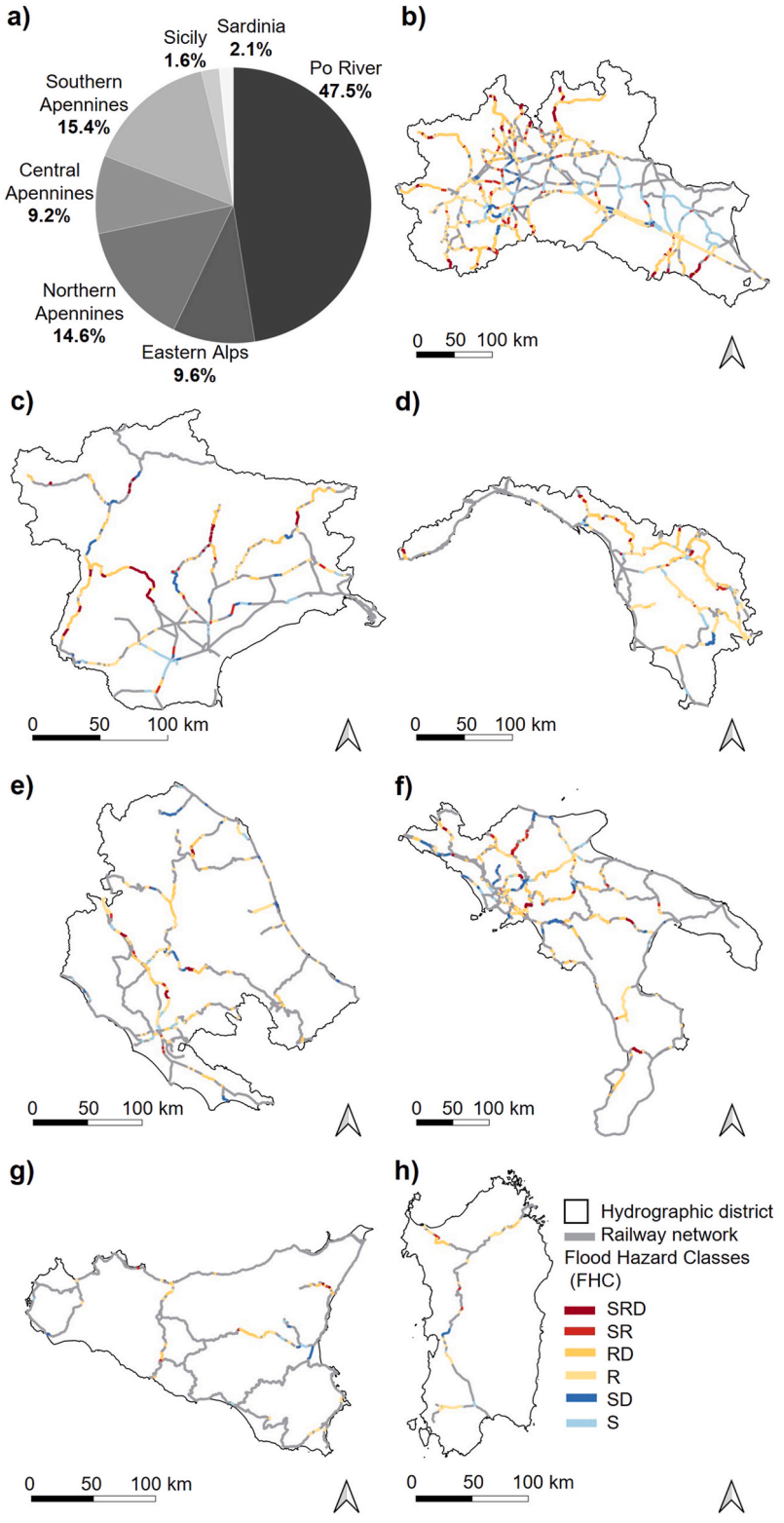

Fig. 7. Identification of flood-prone railway network sections according to the low probability flood hazard scenario (H1). (a) Relative distribution of flood-prone railway network sections across hydrographic districts in Italy, where the overall length of the flood-prone railway network in scenario H1 is equal to 4,523.4 km. Spatial delineation of flood-prone railway network sections according to Flood Hazard Classes (FHCs), for the Po River district (b), Eastern Alps (c), Northern Apennines (d), Central Apennines (e), Southern Apennines (f), Sicily (g) and Sardinia (h).

This reflects the physiographic characteristics of Alpine and Apennine catchments where steep terrain produces both high hillslope gradients (enabling debris-flow proneness) and steeper main channel slopes (resulting in shorter T_c). The consistency of these geomorphological patterns across all flood hazard scenarios demonstrates the significance of both T_c and basin characteristics in the flood hazard classification of railway sections.

Next, we identify the corresponding flood-prone railway sections, whose outlets are represented by the RPs. Also in this case, we show the main outcomes according to the worst-case scenario, i.e., H1 (Fig. 7). Results for H2 and H3 scenarios are provided in the Supplementary Material. The identification of the Flood Hazard Classes (FHCs) characterizing these flood-prone IRN sections shows a clear dominance of Rapid flood processes (Table 2 and Fig. 8). Rapid with Debris (RD) and Rapid no Debris (R) sections make up the largest share, representing 38.5 and 27.3 % of flooded sections (9.9 % and 7 % of the total IRN, respectively). Slow No Debris (S) and Slow with Debris (SD) processes affect a smaller portion of the IRN, constituting 14.9 % and 10.4 % of flooded sections (3.9 % and 2.7 % of the total IRN, respectively, see Table S3 in the Supplementary Tables), while Steep Rapid No Debris (SR) and Steep Rapid with Debris (SRD) processes appear in more limited areas, constituting 4.4 % and 4.5 % of flooded sections (1.1 % and 1.2 % of the total IRN, respectively, see Table S3 in the Supplementary Tables). This pattern is consistently observed across most hydrographic districts, with the majority showing a similar predominance of RD and R classes, particularly evident in the Po River, Northern and Central Apennines. Eastern Alps and Southern Apennines present a slightly larger proportion of S and SD classes. Notably, despite their contrasting geomorphological characteristics, the Po River (27.4 %) and Eastern Alps (29.2 %) districts show similar SD + S percentages, reflecting their internal heterogeneity. The Po River district encompasses both the Po Plain and Alpine/Apennine tributaries, while the Eastern Alps includes major valleys (i.e., Adige, Piave, Brenta rivers) where moderate gradients characterize lower river reaches. Sicily shows a distinctive pattern with a significant presence of SD class as compared to other hydrographic districts. The potential for debris-flow looks relevant, with IRN sections classified as SRD, RD or SD accounting for 42.2 % of the flood-prone IRN for the whole Italian territory.

4. Discussion

A comprehensive flood hazard classification methodology has been proposed and applied to the entire Italian Railway Network (IRN), based on relevant hydrologic and morphologic information such as the contributing area, the river slope and the time of concentration. We acknowledge that several challenges emerged during the analysis. First, the Giandotti formula has been selected as a reference for T_c estimation [29], yet the robustness of our FHC framework has been evaluated through a sensitivity analysis on four alternative formulas. T_c was computed for all 1,756 RPs according to the empirical formulas of Viparelli (1963) [39], Ferro (2006) [40], Pilgrim & McDermott (1981) [41] and Haktanir & Sezen (1990) [42]. These formulas were selected because they exclusively rely on DEM-derived morphological parameters (drainage area A, main channel length L), similarly the Giandotti formula. This ensures a consistent comparison framework where differences in T_c estimates stem solely from the formula structure rather than from additional sources of parameter uncertainty. The calibration ranges of these formulas vary considerably, reflecting different geographical and morphological contexts. Viparelli formula ($T_c = \frac{L}{V}$, with V in m/s) represents an empirical approach with flow velocity V assumed to be equal to 1.5 m/s, consistent with natural river channels [39]. Ferro formula ($T_c = 0.675 \times A^{0.50}$, with T_c in hours and A in km^2) was developed through a multivariate analysis of Italian catchments, with applications spanning areas from 1 to 5,500 km [40]. Pilgrim & McDermott formula ($T_c = 0.76 \times A^{0.38}$) was originally calibrated on 96 rural catchments in Eastern New South Wales, Australia (0.1–250 km^2) [41], and has been extensively validated in Italy across 400 basins with areas ranging from less than 4 km^2 to over 8,

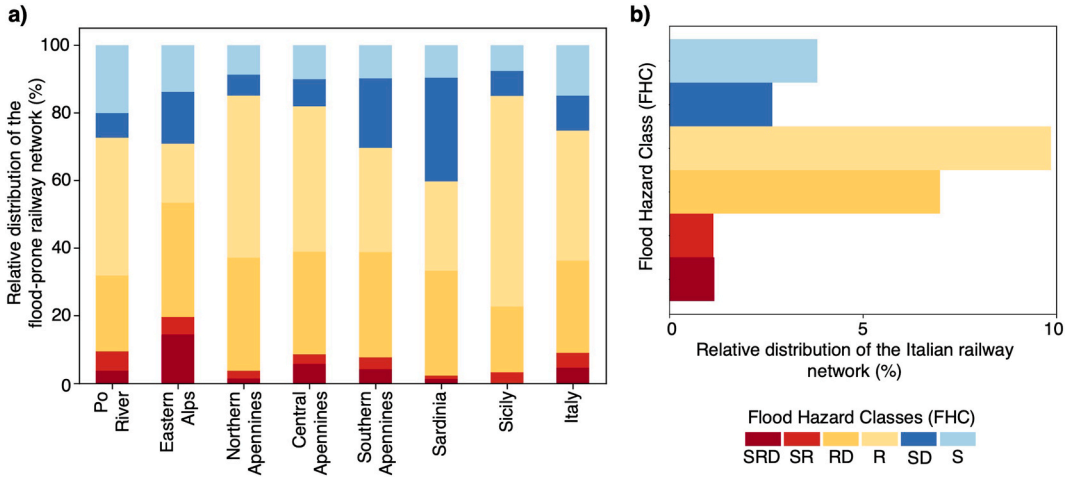

Fig. 8. Relative distribution of Flood Hazard Classes (FHCs) attributed to flood-prone railway network sections according to the low probability flood hazard scenario (H1), with respect to (a) the total length of the flood-prone railway network across hydrographic districts and the entire national territory, (b) the entire railway network, where the overall length is equal to 17,650 km.

000 km^2 [31]. Haktanir & Sezen formula ($T_c = 0.945 \times L^{0.557}$) was originally derived from 10 catchments in Anatolia, Turkey, with areas ranging from 10.6 to 9,867 km^2 and main channel lengths from 5 to 231 km [42]. The Giandotti formula [29], used here as reference, has a calibration range of 170-70,000 km^2. Fig. 9 presents scatter plots comparing T_c estimates from each alternative formula against the Giandotti formulation. The Mean Absolute Percentage Error (MAPE) values quantify systematic deviations: Pilgrim & McDermott shows the lowest MAPE (36.6 %), followed by Viparelli (38.2 %), Ferro (52.6 %), and Haktanir & Sezen (103.5 %). Given the closest agreement with Giandotti, classification changes were analyzed in detail only for Pilgrim & McDermott. The comparison reveals that only 280 out of 1,756 RPs (15.9 %) changed FHC when adopting Pilgrim & McDermott instead of Giandotti. Most changes (270 cases) occurred from Slow (S, SD) to Rapid (R, RD) categories, while only 10 cases moved in the opposite direction, reflecting the systematic tendency of Pilgrim & McDermott to yield shorter T_c estimates. The spatial distribution of classification changes shows no clear geographical pattern, though changes are slightly more frequent in the Po Plain and Apennines, where many basins lie close to the 12-h threshold, which was established collaboratively with RFI based on operational emergency-response criteria. The relative distribution of RPs across flood hazard classes remained statistically stable between the two classifications, indicating that the dominant controls on FHC assignment are preserved regardless of the T_c formula adopted. Our results confirm previous independent outcomes revealing that both Pilgrim & McDermott and Giandotti perform well even beyond their calibration limits [30] and that estimates of T_c values can differ up to half an order of magnitude despite no systematic bias between the two formulas [31]. According to our sensitivity analysis, the Giandotti formula is retained here as reference mainly because it integrates multiple geomorphic parameters (area, length, elevation) providing a comprehensive representation of basin characteristics and because it has been extensively validated in Italian hydrological practice across a wide range of basin scales.

Next, we had to balance computational efficiency with the level of analytical detail in the representation of the intersections between the IRN and the river network. The approach of selecting a single downstream RP for each railway section, while providing consistent assessment criteria, necessarily simplifies these complex interactions. This simplification is supported by the analysis of six test river basins (Paglia, Basento, Aulella, Chienti, Torto, and Dora Baltea) with diverse dimensional and morphological characteristics. For these test basins, we analyzed all river-railway intersections along each railway section, rather than selecting only the most downstream one as we do in the national-scale analysis. This additional analysis demonstrates that most flood-prone railway sections (91.54 %) are shorter than 10 km, with 58.06 % under 5 km. This confirms that the average length of the flood-prone railway sections, even when all sections are considered, does not change significantly. Multiple RPs identified within a 5–10 km distance would add computational complexity without proportional gains in understanding flood dynamics and associated operational processes. Yet, we acknowledge that a comprehensive analysis considering all river-railway intersections at the national scale may represent a valuable development for future research.

Another limitation stems from the reliance on official flood maps [15]. These maps provide standardized coverage across Italy, but they often overlook smaller streams, particularly affecting the characterization of local flooding phenomena in mountainous areas. As discussed in Section 2, FRMP data show substantial heterogeneity in quality, density, and mapping methodology across the seven hydrographic districts [22]. This heterogeneity also affects how RPs are distributed across different areas. The number of RPs depends more on where flood hazard maps actually overlap with railway infrastructure than on the railway network length itself. Areas with extensive railway networks may therefore show relatively few RPs if FRMP coverage does not intersect the railway alignment. These mapping inconsistencies represent a source of uncertainty in our results and highlight the need to carefully identifying FRMP-IRN overlapping zones.

An additional limitation relates to our channel extraction methodology, which relies on a fixed area-slope parameter. While this provides a robust basin-scale approach, it may miss small catchments. The 25 m resolution of EU-DEM [23] presents additional challenges in lowland areas with dense artificial channel networks, such as the Po Plain. In these contexts, the DEM-based approach has difficulty providing the complex drainage patterns created by irrigation canals, embankments, and artificial waterways, leading to inaccuracies in river delineation and in the identification of river-railway intersections. Future applications at local scale could benefit from higher-resolution DEMs (e.g., LiDAR-derived products) and site-specific calibration of threshold parameters. Testing variable thresholds adapted to local physiographic conditions could improve the identification of small flood-prone basins, particularly in areas where railway infrastructure crosses river network. However, such refinements would require careful validation against local hydrographic networks and field observations to avoid introducing spurious drainage patterns, particularly in flat areas where DEM-derived flow directions are more uncertain.

A further consideration concerns the classification thresholds adopted here, which follow the methodological framework by Samela et al. [17], further validated with RFI. These values represent a reasonable compromise between accuracy and computational feasibility at the national scale. While they ensure methodological consistency across Italy, sensitivity testing in representative sub-areas could be valuable to assess potential regional variations and improve classification accuracy in specific contexts. For critical sections identified through this screening approach, however, detailed hydrologic-hydraulic modeling remains necessary to fully characterize flood hazard and support site-specific mitigation design.

Finally, the flood typologies here identified may exhibit varying vulnerability to climate change impacts [43]. Railway sections classified as SRD and SR appear particularly susceptible to the intensification of extreme rainfall due to their short time of concentration, while in areas of moderate slope, the widespread occurrence of RD and R sections raises concerns regarding infrastructure resilience, especially where drainage systems may prove inadequate under high-intensity events [44]. Historical flood loss data across Europe show increasing trends [45], and recent comprehensive analysis demonstrates that floods in small catchments have increased substantially over the past four decades, with increases of 25–30 % closely aligned with a 15 % rise in hourly heavy rainfall [46]. These findings, based on two independent observational networks in Austria, provide robust evidence of a consistent link between sub-daily precipitation extremes and flood dynamics in small basins. The IPCC Sixth Assessment Report further confirms the growing frequency

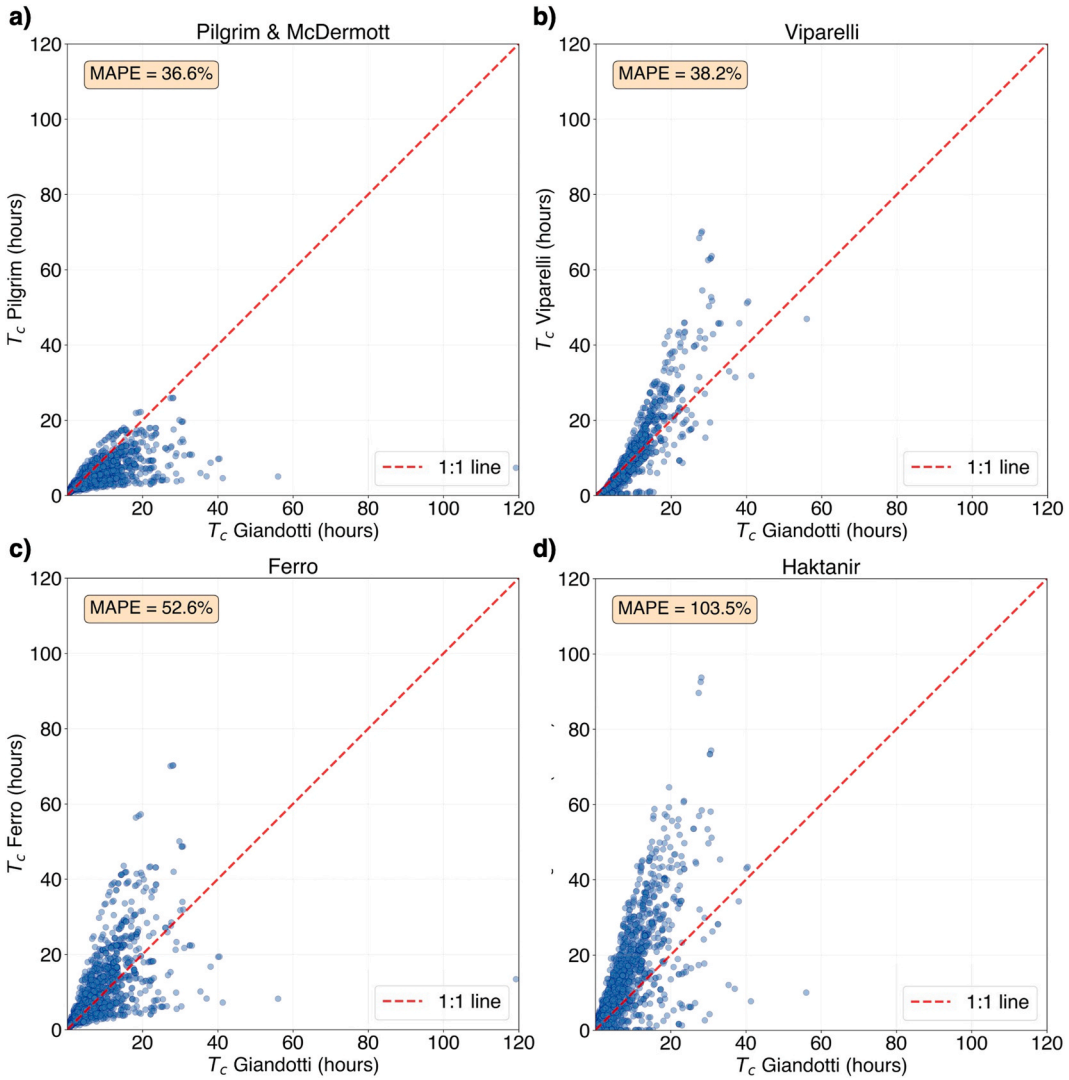

Fig. 9. Scatter plots comparing time of concentration (T_c) estimates from four alternative empirical formulas against the Giandotti formulation for all 1756 Representative Points (H1 scenario). (a) Pilgrim & McDermott: MAPE = 36.6 %. (b) Viparelli: MAPE = 38.2 %. (c) Ferro: MAPE = 52.6 %. (d) Haktanir & Sezen: MAPE = 103.5 %.

and intensity of extreme precipitation events in Southern Europe [47]. These trends are particularly salient in mountainous regions, where the majority of SRD and SR sections are located, as well as in areas with RD and R sections, given that railway-relevant drainage basins tend to have smaller extensions and exhibit rapid response characteristics. The documented intensification of flash flood events in Mediterranean environments is a matter of particular concern [9]. The amplification of flood risks in small, rapidly responding catchments underscores the pressing need for railway-specific adaptation strategies that consider the nonlinear nature of rainfall–runoff processes. In these processes, modest increases in rainfall intensity can result in disproportionately large flood peaks and infrastructure impacts [48].

5. Conclusions

We applied a comprehensive flood hazard classification methodology to the entire Italian Railway Network. This work enables the assessment of flood susceptibility for 17,650 km of infrastructure and creates a consistent database with relevant hydrologic and morphologic information. Our study shows that 25.63 % of the IRN is exposed to potential flooding in the most severe scenario (H1), which decreases to 19.09 % and 9.77 % in the H2 and H3 scenarios. The geographical distribution shows substantial spatial variability. The Po River district accounts for 47.5 % of all flood-prone sections. The classification analysis reveals a clear predominance of rapid flood processes. Over 65 % of flood-prone sections have T_c values shorter than 12 h. Debris-flow proneness affects 42.2 % of exposed infrastructure. This combination of rapid response times and debris-flow potential creates substantial operational challenges for

railway management. We test the robustness of the classification framework through sensitivity analysis on T_c calculations and select the Giandotti formula as our reference. Despite some limitations (i.e., the selection of a single Representative Point per railway section, which simplifies complex river-infrastructure interactions, the reliance on official flood maps, which may overlook smaller streams, particularly in mountainous areas), this work provides railway operators and infrastructure managers with tools for prioritizing interventions and implementing targeted protection measures. Looking ahead, several developments could enhance this methodology. The integration of water depth data from updated flood risk management plans would improve our damage assessment capabilities. Detailed investigation of bridge structures at RPs would better characterize critical infrastructure vulnerabilities to various flood impacts and debris-flows. This approach shows promise for an extension to other linear infrastructures, such as road networks, which could provide a comprehensive transportation infrastructure assessment across Italy, but also across other Mediterranean regions with similar topographical characteristics and flood processes. Finally, the findings derived from this investigation may inform cost-benefit analyses conducted by stakeholders and infrastructure managers in the evaluation and design of alternative infrastructure solutions.

CRediT authorship contribution statement

Gianluca Lelli: Writing – review & editing, Writing – original draft, Visualization, Software, Methodology, Investigation, Formal analysis, Data curation. **Serena Ceola:** Writing – review & editing, Validation, Supervision, Methodology, Conceptualization. **Alessio Domeneghetti:** Writing – review & editing, Validation, Supervision, Methodology, Conceptualization. **Adriana Galli:** Writing – review & editing, Conceptualization. **Edmondo Elisei:** Writing – review & editing, Conceptualization. **Alessandro Rinaldi:** Writing – review & editing, Conceptualization. **Armando Brath:** Writing – review & editing, Validation, Supervision, Methodology, Conceptualization.

Declaration of competing interest

The authors declare that they have no known competing financial interest or personal relationship that could have appeared to influence the work reported in this paper.

Acknowledgements

This study was carried out within the RETURN Extended Partnership, funded by the European Union NextGenerationEU (National Recovery and Resilience Plan – NRRP, Mission 4, Component 2, Investment 1.3 – D.D. 1243 August 2, 2022, PE00000005).

This work was partially supported by Rete Ferroviaria Italiana S.p.A., (research contract n. 2226-2022).

Appendix A. Supplementary data

Supplementary data to this article can be found online at https://doi.org/10.1016/j.ijdrr.2025.105946.

Data availability

Input data sources include freely available and restricted datasets. Flood Risk Management Plans from Italian River Basin Authorities are available at https://idrogeo.isprambiente.it/app/page/open-data. EU-DEM digital elevation model is available at https://www.eea.europa.eu/en/datahub/datahubitem-view/d08852bc-7b5f-4835-a776-08362e2fbf4b. Italian Railway Network data are provided by Rete Ferroviaria Italiana-RFI and are not publicly available. Results from our analysis can be made available upon reasonable request to the authors.

References

[1] E.E. Koks, J. Rozenberg, C. Zorn, M. Tariverdi, M. Vousdoukas, S. Hallegatte, S.A. Fraser, J.W. Hall, A global multi-hazard risk analysis of road and railway infrastructure assets, Nat. Commun. 10 (2019) 2677, https://doi.org/10.1038/s41467-019-10442-3.

[2] M. Pregnolato, A. Ford, S.M. Wilkinson, R.J. Dawson, Impact of flooding and urban adaptation measures on transport network resilience, Transport. Res. Transport Environ. 55 (2017) 239–254, https://doi.org/10.1016/j.trd.2017.06.020.

[3] P. Kellermann, A. Schöbel, G. Kundela, A.H. Thieken, Estimating flood damage to railway infrastructure – the case study of the march river flood in 2006 at the Austrian Northern Railway, Nat. Hazards Earth Syst. Sci. 16 (2016) 2357–2396, https://doi.org/10.5194/nhess-16-2357-2016.

[4] S. Zhu, F. Wang, J. Lv, X. Huang, Q. Zhang, Y. Liu, X. Zhang, Hazard assessment of railway operational safety under flood disasters in China, Nat. Hazards Earth Syst. Sci. 22 (2022) 1519–1534, https://doi.org/10.5194/nhess-22-1519-2022.

[5] D. Mendoza-Tinoco, D. Guan, Z. Zeng, F. Xia, B. Meng, Flood footprint of the 2007 floods in the UK: the case of the affected supply chains, J. Clean. Prod. 168 (2017) 1280–1291, https://doi.org/10.1016/j.jclepro.2017.09.016.

[6] European Environment Agency, European Climate Risk Assessment, European Environment Agency, Copenhagen, 2024. https://www.eea.europa.eu/en/analysis/publications/european-climate-risk-assessment.

[7] P. Bubeck, M. Dillenardt, L. Alfieri, L. Feyen, A.H. Thieken, P. Kellermann, Global warming to increase flood risk on European railways, Clim. Change 155 (2019) 19–36, https://doi.org/10.1007/s10584-019-02434-5.

[8] G. Forzieri, A. Bianchi, F. Batista e Silva, M.A. Marin Herrera, A. Leblois, C. Lavalle, J.C. Aerts, L. Feyen, Escalating impacts of climate extremes on critical infrastructures in Europe, Glob. Environ. Change 48 (2018) 97–107, https://doi.org/10.1016/j.gloenvcha.2017.11.007.

[9] L. Marchi, M. Borga, E. Preciso, E. Gaume, Characterisation of selected extreme flash floods in Europe and implications for flood risk management, J. Hydrol. 394 (2010) 118–133, https://doi.org/10.1016/j.jhydrol.2010.07.017.
[10] S.L. Gariano, F. Guzzetti, Landslides in a changing climate, Earth Sci. Rev. 162 (2016) 227–252, https://doi.org/10.1016/j.earscirev.2016.08.011.
[11] I. Marchesini, O. Althuwaynee, M. Santangelo, M. Alvioli, M. Cardinali, M. Mergili, P. Reichenbach, S. Peruccacci, V. Balducci, I. Agostino, R. Esposito, M. Rossi, National-scale assessment of railways exposure to rapid flow-like landslides, Eng. Geol. 332 (2024) 107474, https://doi.org/10.1016/j.enggeo.2024.107474.
[12] T. Nester, A. Schöbel, U. Drabek, C. Rachoy, H. Wiesenegger, A flood warning system for railways, Georisk 2 (2008) 237–249, https://doi.org/10.1080/17499510802199745.
[13] L. Hong, J. Ouyang, W. Peeta, X. He, Y. Lu, Vulnerability assessment and mitigation for the Chinese railway system under floods, Reliab. Eng. Syst. Saf. 137 (2015) 58–68, https://doi.org/10.1016/j.ress.2014.12.013.
[14] G. Blöschl, J. Hall, A. Viglione, R.A. Perdigão, J. Parajka, B. Merz, D. Lun, B. Arheimer, G.T. Aronica, A. Bilibashi, Others, changing climate both increases and decreases European river floods, Nature 573 (2019) 108–111, https://doi.org/10.1038/s41586-019-1495-6.
[15] A. Trigila, C. Iadanza, B. Lastoria, M. Bussettini, A. Barbano, Dissesto Idrogeologico in Italia: Pericolosità E Indicatori Di Rischio - Edizione 2021, Istituto Superiore per la Protezione e la Ricerca Ambientale, Rome, 2021.
[16] G. Varra, R. Della Morte, M. Tartaglia, A. Fiduccia, A. Zammuto, I. Agostino, C.A. Booth, N. Quinn, J.E. Lamond, L. Cozzolino, Flood susceptibility assessment for improving the resilience capacity of railway infrastructure networks, Water 16 (2024) 2592, https://doi.org/10.3390/w16182592.
[17] C. Samela, F. Carisi, A. Domeneghetti, N. Petruccelli, A. Castellarin, F. Iacobini, A. Rinaldi, A. Zammuto, A. Brath, A methodological framework for flood hazard assessment for land transport infrastructures, Int. J. Disaster Risk Reduct. 85 (2023) 103491, https://doi.org/10.1016/j.ijdrr.2022.103491.
[18] A.-R. Zakaria, T. Oommen, P. Lautala, Automated flood prediction along railway tracks using remotely sensed data and traditional flood models, Remote Sens. 16 (2024) 2332, https://doi.org/10.3390/rs16132332.
[19] G. Watson, S. Ahn, A systematic approach for assessing the effectiveness of flood risk reduction measures for transport infrastructure, Appl. Sci. 12 (2022) 12331, https://doi.org/10.3390/app122312331.
[20] R. Pastorello, T. Michelini, V. d'Agostino, On the criteria to create a susceptibility map to debris flow at a regional scale using Flow-R, J. Mt. Sci. 14 (2017) 621–635, https://doi.org/10.1007/s11629-016-4077-1.
[21] P. Horton, M. Jaboyedoff, B. Rudaz, M. Zimmermann, Flow-R, a model for susceptibility mapping of debris flows and other gravitational hazards at a regional scale, Nat. Hazards Earth Syst. Sci. 13 (2013) 869–885, https://doi.org/10.5194/nhess-13-869-2013.
[22] I. Marchesini, P. Salvati, M. Rossi, M. Donnini, S. Sterlacchini, F. Guzzetti, Data-driven flood hazard zonation of Italy, J. Environ. Manag. 294 (2021) 112986, https://doi.org/10.1016/j.jenvman.2021.112986.
[23] European Environment Agency, EU-DEM v1.1, 2016.
[24] European Environment Agency, EU-Hydro River Network Database 2006-2012, Version 1.3, 2020.
[25] J.F. O'Callaghan, D.M. Mark, The extraction of drainage networks from digital elevation data, Comput. Vis. Graph Image Process 28 (1984) 323–344, https://doi.org/10.1016/S0734-189X(84)80011-0.
[26] D.R. Montgomery, E. Foufoula-Georgiou, Channel network source representation using digital elevation models, Water Resour. Res. 29 (1993) 3925–3934, https://doi.org/10.1029/93WR02463.
[27] F. Giannoni, G. Roth, R. Rudari, A procedure for drainage network identification from geomorphology and its application to the prediction of the hydrologic response, Adv. Water Resour. 28 (2005) 567–581, https://doi.org/10.1016/j.advwatres.2004.11.013.
[28] K.J. Beven, A history of the concept of time of concentration, Hydrol. Earth Syst. Sci. 24 (2020) 2655–2670, https://doi.org/10.5194/hess-24-2655-2020.
[29] M. Giandotti, Previsione delle piene e misurazione delle portate nei piccoli bacini montani. Memorie E Studi Idrografici 5, 1934.
[30] G. Ravazzani, L. Boscarello, A. Cislaghi, M. Mancini, Review of time-of-concentration equations and a new proposal in Italy, J. Hydrol. Eng. 24 (2019) 04019039, https://doi.org/10.1061/(ASCE)HE.1943-5584.0001818.
[31] G. Evangelista, Flood Hazard Sensitivity on Infrastructures in Small Ungauged Watersheds, PhD Thesis, 2023. Politecnico di Torino.
[32] G. Evangelista, R. Woods, P. Claps, Dimensional analysis of literature formulas to estimate the characteristic flood response time in ungauged basins: a velocity-based approach, J. Hydrol. 627 (2023) 130409, https://doi.org/10.1016/j.jhydrol.2023.130409.
[33] D.J. Miller, K.M. Burnett, A probabilistic model of debris-flow delivery to stream channels, demonstrated for the coast range of Oregon, USA, Geomorphology 94 (2008) 184–205, https://doi.org/10.1016/j.geomorph.2007.05.009.
[34] D.R. Montgomery, W.E. Dietrich, A physically based model for the topographic control on shallow landsliding, Water Resour. Res. 30 (1994) 1153–1171, https://doi.org/10.1029/93WR02979.
[35] R. Santos, R. Menéndez Duarte, Topographic signature of debris flow dominated channels: implications for hazard assessment, WIT Trans. Ecol. Environ. 90 (2006) 143–152, https://doi.org/10.2495/DEB060291.
[36] D. Rickenmann, M. Zimmermann, The 1987 debris flows in Switzerland: documentation and analysis, Geomorphology 8 (1993) 175–189, https://doi.org/10.1016/0169-555X(93)90036-2.
[37] T. Takahashi, Debris Flow: Mechanics, Prediction and Countermeasures, Taylor & Francis, London, 2007, https://doi.org/10.1201/9780203946282.
[38] A. Blais-Stevens, P. Behnia, Debris flow susceptibility mapping using a qualitative heuristic method and Flow-R along the Yukon Alaska Highway Corridor, Canada, Nat. Hazards Earth Syst. Sci. 16 (2016) 449–462, https://doi.org/10.5194/nhess-16-449-2016.
[39] C. Viparelli, Apporti idrici superficiali in Campania, in: Supplemento Agli Annali Dei Lavori Pubblici, n. 12, Istituto di Idraulica, Università di Palermo, Italy, 1961.
[40] V. Ferro, Riqualificazione ambientale dei corsi d'acqua, in: Quaderni Di Idronomia Montana. Giardini Naxos, Italy: Nuova Editoriale Bios, 2006.
[41] D.H. Pilgrim, Travel times and nonlinearity of flood runoff from tracer measurements on a small watershed, Water Resour. Res. 12 (1976) 487–496, https://doi.org/10.1029/WR012i003p00487.
[42] T. Haktanir, N. Sezen, Suitability of two-parameter gamma and three-parameter beta distributions as synthetic unit hydrographs in Anatolia, Hydrol. Sci. J. 35 (1990) 167–184, https://doi.org/10.1080/02626669009492416.
[43] S. Hettiarachchi, C. Wasko, A. Sharma, Increase in flood risk resulting from climate change in a developed urban watershed – the role of storm temporal patterns, Hydrol. Earth Syst. Sci. 22 (2018) 2041–2056, https://doi.org/10.5194/hess-22-2041-2018.
[44] F. Nemry, H. Demirel, Impacts of Climate Change on Transport: a Focus on Road and Rail Transport Infrastructures, European Commission Joint Research Centre, Luxembourg, 2012, https://doi.org/10.2791/15504.
[45] D. Paprotny, A. Sebastian, O. Morales-Nápoles, S.N. Jonkman, Trends in flood losses in Europe over the past 150 years, Nat. Commun. 9 (2018) 1985, https://doi.org/10.1038/s41467-018-04253-1.
[46] K. Haslinger, K. Breinl, L. Pavlin, Others, increasing hourly heavy rainfall in Austria reflected in flood changes, Nature 639 (2025) 667–672, https://doi.org/10.1038/s41586-025-08647-2.
[47] IPCC, Climate Change 2022: Impacts, Adaptation and Vulnerability, Intergovernmental Panel on Climate Change, Geneva, 2022, https://doi.org/10.1017/9781009325844.
[48] M. Bertola, A. Viglione, D. Lun, J. Hall, G. Blöschl, Flood trends in Europe: are changes in small and big floods different? Hydrol. Earth Syst. Sci. 24 (2020) 1805–1822, https://doi.org/10.5194/hess-24-1805-2020.